



**HAL**  
open science

# Investigation of emission heterogeneity in InGaN/GaN micro-LEDs by photon-correlation cathodoluminescence spectroscopy

Pablo Sáenz de Santa María Modroño, Corentin Le Maoult, Nicolas Bernier,  
David Vaufrey, Gwénoél Jacopin

► **To cite this version:**

Pablo Sáenz de Santa María Modroño, Corentin Le Maoult, Nicolas Bernier, David Vaufrey, Gwénoél Jacopin. Investigation of emission heterogeneity in InGaN/GaN micro-LEDs by photon-correlation cathodoluminescence spectroscopy. ACS photonics, In press, 10.1021/acsphotonics.4c00300 . hal-04585936

**HAL Id: hal-04585936**

**<https://hal.science/hal-04585936>**

Submitted on 23 May 2024

**HAL** is a multi-disciplinary open access archive for the deposit and dissemination of scientific research documents, whether they are published or not. The documents may come from teaching and research institutions in France or abroad, or from public or private research centers.

L'archive ouverte pluridisciplinaire **HAL**, est destinée au dépôt et à la diffusion de documents scientifiques de niveau recherche, publiés ou non, émanant des établissements d'enseignement et de recherche français ou étrangers, des laboratoires publics ou privés.

# Investigation of emission heterogeneity in InGaN/GaN micro-LEDs by photon-correlation cathodoluminescence spectroscopy

Pablo Sáenz de Santa María Modroño<sup>1</sup>, Corentin Le Maoult<sup>2</sup>, Nicolas Bernier<sup>2</sup>, David Vaufrey<sup>2</sup>, Gwénolé Jacopin<sup>1\*</sup>

<sup>1</sup> Univ. Grenoble Alpes, CNRS, Grenoble INP, Institut Néel, 38000 Grenoble, France

<sup>2</sup> Univ. Grenoble Alpes, CEA-LETI, Grenoble INP, 38000 Grenoble, France

E-mail: gwenole.jacopin@cnrs.fr

Feb 2024

**Abstract.** The emission properties of InGaN/GaN  $\mu$ -LEDs of different sizes and shapes have been investigated by spectrally-resolved and time-correlated cathodoluminescence spectroscopy. This approach provides high spatial and temporal resolution, allowing us to simultaneously measure CL spectra and carrier lifetime at the single  $\mu$ -LED level. It also enables us to investigate the correlation between these parameters within individual  $\mu$ -LEDs and across multiple devices. Our observations show a large variation in CL intensity between similarly sized  $\mu$ -LEDs, particularly in the smallest samples. This variation correlates with changes in emission wavelength and has been attributed to differences in injection efficiency between samples, caused by V-pit type defects in the active region.

## Keywords

Carrier dynamics, InGaN, cathodoluminescence, light-emitting diodes, time-resolved spectroscopy, V-pits

## 1. Introduction

Over the past two decades, lighting has undergone a revolutionary transformation with the advent of GaN-based light emitting diodes (LED) technology. These LEDs are characterized by their remarkable efficiency, exceptionally long operational lifespans,<sup>1</sup> and a tunable bandgap that allows the emission over a wide spectral ranges. More recently, industrial and academic players have proposed the use of GaN  $\mu$ -LEDs for microdisplay applications. These future displays could benefit from the unmatched luminance of GaN based  $\mu$ -LEDs.<sup>2</sup> However, a number of technological barriers need to be overcome in order to move from efficient LEDs to commercially viable  $\mu$ -LED displays. One of the biggest challenges is to maintain the high external quantum efficiency when switching from large LEDs to  $\mu$ -LEDs,<sup>3,4</sup> although recently a technique name neutral beam etching has been shown to achieve minimal loss of quantum efficiency for square  $\mu$ LEDs as small as 3.5  $\mu\text{m}$ .<sup>5</sup> Another challenge is maintaining uniform brightness and color from pixel to pixel.<sup>6</sup>

## 2. Experimental methods

In this work, we studied the optical properties of individual blue InGaN/GaN  $\mu$ -LEDs of sizes ranging from 1 to 50  $\mu\text{m}$  using spatially and spectrally resolved cathodoluminescence (CL) spectroscopy. In addition to the standard CL spectroscopy, we simultaneously probed the carrier lifetime of each  $\mu$ -LED using spatially resolved Hanbury-Brown-Twiss (HBT) interferometry measurements.

The samples were etched from a commercial blue LED, and were given a surface passivation treatment. The details of this treatment can be found in chapter 5 of the following work<sup>7</sup> (pg 155), where our sample was labelled "sample T". The process consisted on in-situ N<sub>2</sub>H<sub>2</sub> plasma nitridation pre-treatment, followed by AlN/Al<sub>2</sub>O<sub>3</sub> bi-layer passivation.

All measurements were performed in a FEI Inspect F50 scanning electron microscope (SEM).<sup>8</sup> The light was collected using a parabolic mirror and separated in two beams with a 50/50 beamsplitter. One of the beams was measured with a spectrometer and the other with the HBT setup. This configuration allows us to simultaneously obtain SEM and spatially resolved CL images as well as carrier lifetime at the nanoscale. The experimental setup is described in more detail in.<sup>9</sup>

More than a 150 different individual  $\mu$ LEDs were studied, with both square and circular shapes. The sample structure (from top to bottom) is as follows: An upper layer of p-GaN (80 nm); an AlInGaN superlattice (80 nm) on top of another p-GaN layer (40 nm), an electron blocking layer (EBL) on AlGaIn (20 nm); a multiple quantum well (MQW) structure

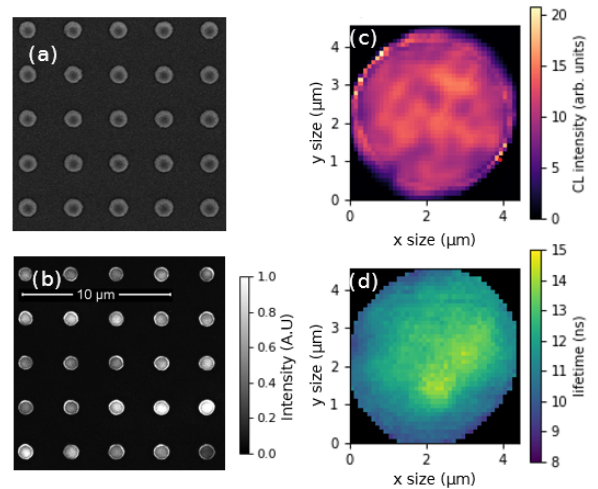


**Figure 1.** (a-b) Secondary electron microscope (SEM) (a) and simultaneously acquired spatially resolved CL (b) images of circular  $\mu$ LEDs with a diameter of about 1.3  $\mu\text{m}$ . The images were obtained with an acceleration voltage of 10 kV and a e-beam current of 14 pA. The CL image shows intensity for wavelengths in the  $440 \pm 20$  nm range. Scale bar is the same for both images. (c-d) Spatially resolved CL intensity (c) and effective lifetime (d) for a 4  $\mu\text{m}$  circular  $\mu$ LED.

of 15 nm of GaN on top of 3nm of InGaN, repeated nine times; an underlayer structure of GaN (15 nm) on top of InGaN (6.5 nm) repeated six times; a layer of nominally undoped GaN (200 nm); and finally a thick layer (2100 nm) of n-GaN on top a the sapphire substrate.

Unlike previous studies on  $\mu$ -LEDs, which either focus on individual pixels<sup>10,11</sup> or average large regions,<sup>12</sup> we focus on the study and comparison of pixel-to-pixel emission properties.

As depicted in figure 2 (a,b), adjacent pixels of nominally identical size and shape can exhibit significant variations in CL brightness. This behaviour was observed in every collection of  $\mu$ LEDs examined, with the brighter pixels reaching twice the intensity of the darker ones in the most extreme cases. As mentioned above, this could represent a major problem to display applications as the pixel yield has to be maintained above 99.9999% to mitigate the probability of dead pixels in 4 K displays.<sup>13</sup>

## 3. Results and discussion

In order to study the origin of this difference in intensity, we first investigated the local variation of photon emission statistics with an HBT interferometer. This setup uses a 50/50 beamsplitter, two single photon detectors, and a correlator to estimate the auto-correlation function  $g^2(\tau)$  of the CL light source. This function  $g^2(\tau)$  is the probability of detecting a photon at a time  $t + \tau$  in one of the detectors given that a

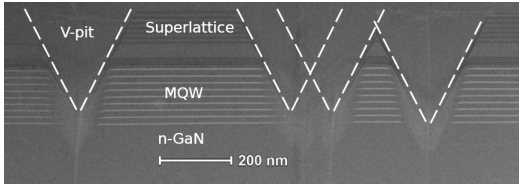


**Figure 2.** STEM image of a vertical cut from one of our  $\mu$ LED pixels. Detail on the measurement conditions can be found in.<sup>7</sup> The studied mesa is a  $2.5 \mu\text{m}$  square. Sample was prepared with focused ion beam etching to obtain a width of  $80 \text{ nm}$ . Four V-pits can be seen in the active region.

photon was detected on the other one at time  $t$ .<sup>14</sup> The light beam was spectrally filtered via a bandpass filter ( $400 - 500 \text{ nm}$ ) before the HBT to analyse only the active region emission range. The purpose of HBT measurements is to determine the carrier lifetime inside the QW region. Indeed, since a single SEM electron generates almost instantaneously hundreds of electron-hole pairs, the subsequent light emission will follow a super-Poissonian distribution.<sup>15</sup> It can be demonstrate that the temporal extension of this photon bunch is directly linked to the carrier lifetime. In fact, carrier lifetime can be estimated from the auto-correlation function by simply fitting it to an exponential decay.<sup>16</sup>

The main drawback of the HBT technique is the requirement the photon bunches do not overlap. To achieve this, the time between the arrival of two electrons needs to be significantly larger than the carrier lifetime. This puts a hard cap on the current, therefore all the measurements have been done in the low current regime.

As the extracted local carrier lifetime is proportional to the Internal Quantum Efficiency (IQE), we can thus directly map the local IQE variation, which is nearly independent of extraction efficiency (EXE) and injection efficiency (IE). This is in stark contrast to the CL intensity, which is also a function of both EXE and IE.

The HBT setup allows for the carrier lifetime and the CL intensity to be measured simultaneously. Therefore, a change in intensity that does not correlate with a change in lifetime indicates a change in either extraction or injection efficiency.

Figure 2 (c,d) shows both intensity and carrier lifetime mapping of a single circular  $4 \mu\text{m}$   $\mu$ LED. Such a mapping were acquired using a dwell time of  $0.5$  seconds per pixel while the time binning was set to  $32 \text{ ps}$ . The particular  $\mu$ LED shown in the image had a large intensity for pixels of this size and shape,  $30 \%$  above average. In the CL lifetime mapping, we observe a decrease in lifetime near the edges of the pixels, evidencing the detrimental role of surface recombinations on the  $\mu$ LED IQE, and was already observed by previous studies.<sup>9,17</sup> Similar mappings for

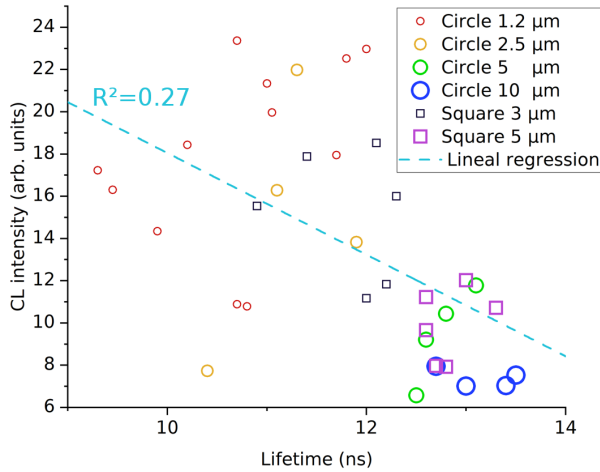
multiple  $\mu$ LEDs can be found in the supplementary materials. The increase in CL intensity near the edge is attributed to the increased overlap between the CL excitation area and the active region.<sup>17</sup> The extra brightness of the edge seems concentrated in two opposing extremes, which is likely an artifact induced by SEM astigmatism.

Figure 2(c) also shows dark spots in the CL intensity that do not correlate with a change in lifetime. Similar results were obtained for all  $\mu$ LEDs. This suggests a local effect that affects either the EXE or the IE, but not the IQE.

To determine what type of defect could be responsible for such dark spots, we then performed scanning transmission electron microscope (STEM) imaging on  $\mu$ LEDs. As shown in Figure 2, we were able to identify the presence of four V-pits within a single mesa, which drastically affect the heterostructure in the vicinity of the active region. The density of the V-pits was not uniform, with all of the V-pits concentrated in one half of the mesa. Figure 2 is a zoom in of said area to better display the effect of V-pits on the heterostructure. We have therefore investigated the possibility that the V-shaped wells formed around the dislocations<sup>18,19</sup> are at the origin of these intensity changes.

As proposed by Hangleiter *et al.*,<sup>20</sup> V-pits create a energy barrier around the local defect. While the dislocation creates a non-radiative decay path, but e-h pairs generated outside the V-pit can not reach it due to the barrier. Meanwhile, e-h pairs created directly in the V-pit almost instantaneously recombine non-radiatively on the dislocation<sup>19</sup> and do not contribute to CL intensity. Consequently, they do not influence the local carrier lifetime. The final result is a de facto decrease in injection efficiency near the V-pit, as only e-h pairs outside of it can emit a photon and be detected.

We then estimate the density of V-pits by counting the amount of dark points in a CL image of a large non-etched region of the LED. The number of V-pits was estimated by a program that tested for circular regions that were both darker than their surroundings and rotationally symmetrical. This CL image with the V-pit count can be found in the supplementary materials. We approximated the density to be around  $7.6 \pm 0.1 \cdot 10^8 \text{ Vpits} \cdot \text{cm}^{-2}$ . This value matches the amount expected from figure 2 ( $2 \pm 1 \cdot 10^9 \text{ Vpits} \cdot \text{cm}^{-2}$ ), but is larger than previous reports for the expected V-pit density of InGaN LEDs grown on sapphire, of  $1.5 \cdot 10^8 / \text{cm}^2$ <sup>21</sup> and  $3 - 5 \cdot 10^8 / \text{cm}^2$ .<sup>22</sup> However, as observed by,<sup>23</sup> the amount of V-pits grows with the number of layers, so that discrepancy could be explained by the presence of an underlayer. As observed on the STEM images, the V-pits cannot be counted by high resolution SEM nor atomic force microscopy due to the



**Figure 3.** Intensity vs lifetime at the center of the  $\mu$ LED for an acceleration voltage of 10 kV and a current of 14 pA. There is a low negative of correlation between intensity and lifetime. There is also a negative correlation between the lifetime and the pixel size, with smaller pixels having shorter lifetimes.

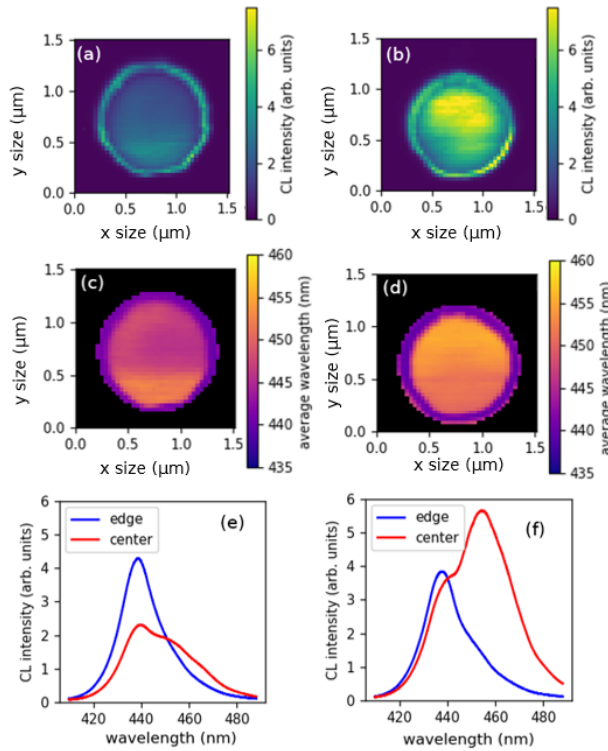


**Figure 4.** Spatially resolved CL spectra of two distinct  $\mu$ LED pixels, with low (left) and high (right) intensity. The pixels were adjacent, had similar sizes and shapes, and were studied under the same beam conditions. Figures (a) and (b) show the spatial distribution of total MQW CL Intensity, figures (c) and (d) show the average wavelength for the spectra at each point, and (e) and (f) show the average spectra at the center and edge of the  $\mu$ LED.

conformal growth of the p-GaN layer.

To better understand the influence of such defects on the efficiency of  $\mu$ LED, we performed HBT measurements on pixels of multiple sizes. The results can be seen in figure 3. It is important to note that both CL intensity and carrier lifetime will depend on a series of factors, including acceleration voltage and probe current,<sup>18</sup> which were modified for different measurements to study their effect in the  $\mu$ LEDs. Hence, only measurements performed under the exact same conditions (acceleration voltage 10 kV, beam current 14 pA, room temperature) are displayed in the graph.

The graph does show a negative correlation ( $R^2 = 0.27$ ) between CL intensity and carrier lifetime, which is the opposite of what would be expected if the change in CL intensity was related to an IQE variation. However, this can be explained by the different sizes of  $\mu$ LEDs studied. Within pixels of the same size, the correlation is positive, but smaller pixels have larger intensity and lower lifetime. The lower lifetime is probably due to surface recombination, and the higher intensity indicates that the extraction efficiency is favored in small  $\mu$ LEDs, due to the extra surface provided by the sidewalls, as seen by Olivier *et al.*<sup>24</sup> For the smallest pixels, the presence of resonant cavity modes such as whispering gallery mode may also contribute to the enhancement of the light emission.<sup>25</sup>

Light extraction efficiency is a key issue for GaN LED applications. The reason is the high refractive index of GaN, of about 2.48. This means the critical angle for an GaN/air interface is about  $24^\circ$ , which causes a large part of the light to reflect back inside the LED. The edge provides a second interface that allows extra photons to escape, hence the larger luminosity of smaller LEDs. Different solutions have been proposed to overcome this low extraction efficiency, like reducing sample size,<sup>26</sup> or the work by Ley *et al.*,<sup>27</sup> which uses a structure with mirrors on the sidewalls to illuminate the backside of the LED.

The interaction between surface recombination and extraction efficiency at difference sizes has been recently studied by González-Izquierdo *et al.*<sup>26</sup> Notably, their study shows that, in the case of samples without surface passivation the optimal size is reached at 5  $\mu$ m in width, as the effect of surface recombination surpasses extraction efficiency growth below that size. In our samples with surface passivation, the effect of the edge in the IQE is lessened, which means the optimal size is smaller. In fact, we are unable to determine optimal size for our  $\mu$ LEDs because our intensity grows as size decreases up to the smallest size of 1.2  $\mu$ m.

Figure 3 demonstrates that there is a variation in lifetime and intensity from pixel to pixel, even between similarly sized ones. This variation is particularly

pronounced in smaller  $\mu$ LEDs. The change in lifetime, however, is rather small ( $\pm 20\%$ ) compared to the variation in intensity ( $\pm 100\%$ ), and the correlation between the two is not significant. This shows that the differences in IQE between pixels have a small effect on the intensity compared with injection and extraction efficiency.

The study done by González-Izquierdo,<sup>26</sup> didn't observe a meaningful variation in intensity between similarly sized samples at low temperature. Their samples were not surface passivated, and the study was done at low temperature, but none of those differences should affect the extraction efficiency, since it mostly depends on the refractive index, which barely changes for GaN at low T.<sup>28</sup> Hence, injection efficiency must be the underlying source of variation.

Furthermore, as discussed by,<sup>26</sup> defect states are frozen at 10 K. The fact that<sup>26</sup> did not find significant differences in intensity between same-sized pixels and this study did is consistent with the V-pit explanation. The larger intensity variation in smaller LEDs also supports this explanation. The smallest pixels have a surface of about  $1 \mu\text{m}^2$ , so they will contain only one V-pit on average. Therefore, the number of V-pits per  $\mu$ LEDs may vary significantly ranging from 0 to a few, since the pixels were etched post growth. Hence, despite a high V-pit density, it is statistically possible to obtain single  $\mu$ LED free from V-pits.

When studying the spatially resolved CL spectra, we found the  $\mu$ LED properties to range between two distinct behaviours from these two extreme types of pixels, which are shown in figure 4.

$\mu$ LEDs with larger intensity were red-shifted and brighter in the center, while pixels with lower intensity were less bright and blue-shifted at the center. The edge was always blue-shifted, regardless of the kind of pixel, confirming results by Xie *et al.*<sup>10</sup> and Zhang *et al.*,<sup>12</sup> which attributed the edge blue-shift to strain relaxation. Smaller  $\mu$ LEDs have a larger edge to surface ratio, hence edge emission will represent a larger fraction of their total intensity. The measured spectra appear to have two peaks at fixed values, which we believe are caused by optical resonances. This is due to the fact that the two peaks appear at the interference maxima for a 2800 nm GaN layer, and in fact there was almost no difference in error rate when fitting the spectra to a single Gaussian with interference effects versus a pair of Gaussians with similar interference.

Within individual pixels, red-shifted areas outside the edge are brighter as well. Smaller pixels are more likely to be red-shifted, which relates to their larger range of possible intensities. Smaller pixels and squares are also brighter than other pixels with similar average wavelength due to the larger edge to surface ratio.

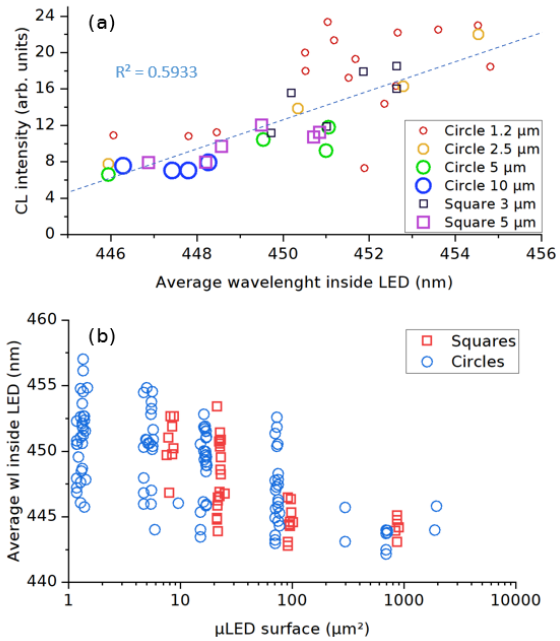


**Figure 5.** (a) CL intensity as a function of arithmetic mean emission wavelength at the center of the  $\mu$ LED for an acceleration voltage of 10 kV and a current of 0.014 nA. (b) Arithmetic mean emission wavelength at the center of the  $\mu$ LED as a function of the  $\mu$ LED area.

Figure 5 illustrates this relation between intensity, red-shift and size. Average wavelength emission, unlike intensity or lifetime, was not found to be dependent on SEM current, hence all the  $\mu$ LEDs are displayed in Figure 5 (b). The positive correlation seen in figure 5 (a) was similarly observed for different conditions, which can be found in the supplementary materials.

Since there is no correlation between wavelength shift and lifetime, there must be a mechanism that affects the EQE and the spectra, but not the IQE. It has been observed by Chen *et al.*<sup>29</sup> that V-pits can alter the emission properties of LEDs during operation, with wavelength decreasing as total V-pit surface increases. V-pits cause strain relaxation,<sup>30</sup> which could cause a blue-shift in the surrounding QW emission, similarly to the edge. Also, as mentioned before, V-pits do not affect the measured lifetime. These properties match our observations, supporting the role of V-pits in the CL intensity variation. Pixels with a larger V-pit concentration are blue-shifted, as shown by,<sup>29</sup> and their total intensity is lower, due to their detrimental effect in injection efficiency, since e-h pairs created inside a V-pit do not contribute to intensity, as per,<sup>19</sup> explaining the correlation seen in figure 5.

Figure 5 shows that both the total intensity and emission wavelength change significantly from pixel to pixel in the smaller  $\mu$ LEDs, while averaging out on the bigger ones. The number of V-pits inside a single

$\mu$ LED therefore needs to variate a lot from pixel to pixel for our explanation to be correct. Figure 5 (b) also shows that smaller samples are overall blue-shifted in relation to larger ones. This can be explained by the edge blue-shift observed in figure 4. Smaller samples have a larger contribution from the edge to their total intensity, even when exciting e-h pairs outside the edge, due to both carrier mobility and the excitation volume of the electron beam.

The rather low amount of V-pits inside single  $\mu$ LEDs means that variance on their concentration between samples will be large, specially on smaller pixels. This matches the results from figure 5, which shows a larger intensity and wavelength shift between smaller  $\mu$ LEDs. Hence, V-pits are the most likely candidate for the source of CL intensity variation between pixels.

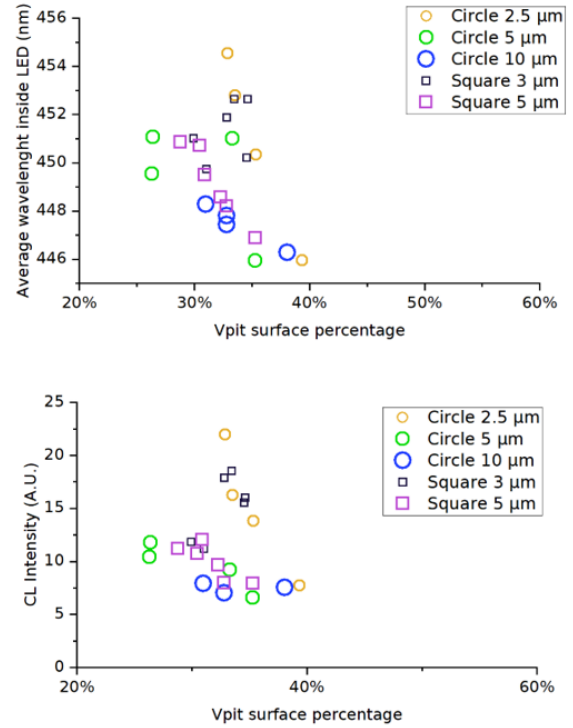
As a final test to the V-pit explanation for the emission heterogeneity between  $\mu$ LEDs, we decided to study the relationship between their concentration, intensity and wavelength. Since V-pits can have different sizes, as shown in the additional materials, we decided to estimate the fraction of the total surface of the LED they represented. In order to do this we considered that a point within the CL mapping of a  $\mu$ LED was a V-pit if its intensity was less than 95% of the average emission of the  $\mu$ LED. The additional materials show examples of this selection process.

Figure 6 shows the correlation between this percentage and both intensity and wavelength. The smallest  $\mu$ LEDs were not included due to the difficulty of measuring the V-pits due to their large effect on average intensity, since a large V-pit could fully cover a small sample. The trend is clear: Darker  $\mu$ LEDs are not uniformly darker, they are darker on only some parts of their surface. Similarly, blue shifted  $\mu$ LEDs have a larger percentage of darker regions. Both of these results match the V-pit explanation.

V-pits are usually considered a desirable defect for large nitride LEDs.<sup>31</sup> First, they do not affect the EQE because of the potential barrier between the active region and the dislocation. Second, they can even improve the wall plug efficiency by lowering the forward voltage in InGaN/GaN LEDs due to lateral hole injection.<sup>32</sup> In contrast, our results show that, for  $\mu$ LEDs, V-pits can induce a color and intensity variation from pixel to pixel, which may be caused by strain relaxation.

#### 4. Conclusion

We have studied the properties of a large number of  $\mu$ LEDs using spatially resolved and time-correlated CL. We have found that light emission can change by a factor of two between seemingly identical  $\mu$ LEDs.



**Figure 6.** (Top) Average wavelength and (bottom) Percentage of V-pit surface in pixel (defined as percentage of  $\mu$ LED pixel surface with intensity below 95% of average LED intensity).

We have mapped the lifetime of multiple pixels and found no correlation within single  $\mu$ LEDs between lifetime and intensity. This points out to a significant variation in either extraction or injection efficiency within individual pixels. The source of this variation has been attributed to differences in the V-pit number between pixels.

Between different  $\mu$ LEDs, variations in intensity were correlated with a change in wavelength at the center of the pixels, with less bright  $\mu$ LEDs blue-shifted. This blue-shift has also been attributed to the increased concentration of V-pits due to its negative correlation with CL intensity. This matches previous observations on the effect of V-pits on emission wavelength. Smaller pixels had a higher range of possible values for intensity, lifetime, and red-shift, which has been attributed to the larger expected variance on the amount of V-pits.

#### 5. Acknowledgements

This work is supported by the French National Research Agency in the framework of the INDIANA Project No. ANR-21-CE42-0020-01 and with the help of the “Plateforme Technologique Amont” de Grenoble, with the financial support of CNRS Renatech network. The authors would like to thank

Fabrice Donatini for his help in the development of the SRTC-CL setup and Audrey Jannaud for TEM lamella preparation.

## References

- [1] Matteo Buffolo et al. “Defects and Reliability of GaN-Based LEDs: Review and Perspectives”. In: *physica status solidi (a)* 219.8 (2022), p. 2100727. DOI: <https://doi.org/10.1002/pssa.202100727>. eprint: <https://onlinelibrary.wiley.com/doi/pdf/10.1002/pssa.202100727>. URL: <https://onlinelibrary.wiley.com/doi/abs/10.1002/pssa.202100727>.
- [2] Jung-El Ryu et al. “Technological Breakthroughs in Chip Fabrication, Transfer, and Color Conversion for High-Performance Micro-LED Displays”. In: *Advanced Materials* 35.2204947 (Feb. 2023). DOI: 10.1002/adma.202204947.
- [3] Sergey Konoplev, Kirill Bulashevich, and Sergey Karpov. “From Large-Size to Micro-LEDs: Scaling Trends Revealed by Modeling”. In: *physica status solidi (a)* 215.1700508 (Dec. 2017). DOI: 10.1002/pssa.201700508.
- [4] François Olivier et al. “Influence of size-reduction on the performances of GaN-based micro-LEDs for display application”. In: *Journal of Luminescence* 191 (Sept. 2016), pp. 112–116. DOI: 10.1016/j.jlumin.2016.09.052.
- [5] Xuelun Wang et al. “ $3.5 \times 3.5 \mu\text{m}^2$  GaN blue micro-light-emitting diodes with negligible sidewall surface nonradiative recombination”. In: *Nature Communications* 14.1 (Nov. 2023), p. 7569. ISSN: 2041-1723. DOI: 10.1038/s41467-023-43472-z. URL: <https://doi.org/10.1038/s41467-023-43472-z>.
- [6] Kai Ding et al. “Micro-LEDs, a Manufacturability Perspective”. In: *Applied Sciences* 9.6 (2019), p. 1206. ISSN: 2076-3417. DOI: 10.3390/app9061206. URL: <https://www.mdpi.com/2076-3417/9/6/1206>.
- [7] Corentin Le Maoult. “Etude et optimisation de l ’ étape de passivation des  $\mu\text{LED}$  bleues GaN-InGaN”. PhD thesis. Université Grenoble Alpes, 2021. URL: <https://www.theses.fr/2021GRALT073>.
- [8] *FEI Company - Inspect™ Community, Manuals and Specifications — LabWrench*. URL: <https://www.labwrench.com/equipment/7220/fei-company-inspect-trade>.
- [9] Sylvain Finot. “Cathodoluminescence lifetime spectroscopy for efficient III-nitride LEDs”. PhD thesis. Université Grenoble Alpes, 2022. URL: <https://www.theses.fr/2022GRALY064>.
- [10] E. Y. Xie et al. “Strain relaxation in In-GaN/GaN micro-pillars evidenced by high resolution cathodoluminescence hyperspectral imaging”. English. In: *Journal of Applied Physics* 112.1 (July 2012), p. 013107. ISSN: 0021-8979. DOI: 10.1063/1.4733335.
- [11] Jinglin Zhan et al. “Investigation on strain relaxation distribution in GaN-based  $\mu\text{LEDs}$  by Kelvin probe force microscopy and micro-photoluminescence”. In: *Opt. Express* 26.5 (Mar. 2018), pp. 5265–5274. DOI: 10.1364/OE.26.005265. URL: <https://opg.optica.org/oe/abstract.cfm?URI=oe-26-5-5265>.
- [12] Chaoqiang Zhang et al. “Strain Relaxation Effect on the Peak Wavelength of Blue InGaN/GaN Multi-Quantum Well Micro-LEDs”. In: *Applied Sciences* 12.15 (2022), p. 7431. ISSN: 2076-3417. DOI: 10.3390/app12157431. URL: <https://www.mdpi.com/2076-3417/12/15/7431>.
- [13] Chien-Chung Lin et al. “The micro-LED roadmap: status quo and prospects”. In: *Journal of Physics: Photonics* 5.4 (2023), p. 042502. DOI: 10.1088/2515-7647/acf972.
- [14] Roy J. Glauber. “The Quantum Theory of Optical Coherence”. In: *Phys. Rev.* 130 (6 June 1963), pp. 2529–2539. DOI: 10.1103/PhysRev.130.2529. URL: <https://link.aps.org/doi/10.1103/PhysRev.130.2529>.
- [15] Tatsuro Yuge et al. “Superbunching in cathodoluminescence: A master equation approach”. In: *Phys. Rev. B* 107 (16 2023), p. 165303. DOI: 10.1103/PhysRevB.107.165303. URL: <https://link.aps.org/doi/10.1103/PhysRevB.107.165303>.
- [16] Sophie Meuret et al. “Nanoscale Relative Emission Efficiency Mapping Using Cathodoluminescence  $g(2)$  Imaging”. In: *Nano Letters* 18.4 (2018). PMID: 29546762, pp. 2288–2293. DOI: 10.1021/acs.nanolett.7b04891. eprint: <https://doi.org/10.1021/acs.nanolett.7b04891>. URL: <https://doi.org/10.1021/acs.nanolett.7b04891>.
- [17] Sylvain Finot et al. “Surface Recombinations in III-Nitride Micro-LEDs Probed by Photon-Correlation Cathodoluminescence”. In: *ACS Photonics* 9.1 (2022), pp. 173–178. DOI: 10.1021/acsp Photonics.1c01339. eprint: <https://doi.org/10.1021/acsp Photonics.1c01339>. URL: <https://doi.org/10.1021/acsp Photonics.1c01339>.



- [18] Aurelien David. “Long-Range Carrier Diffusion in (In, Ga)N Quantum Wells and Implications from Fundamentals to Devices”. In: *Phys. Rev. Appl.* 15 (5 May 2021), p. 054015. DOI: 10.1103/PhysRevApplied.15.054015. URL: <https://link.aps.org/doi/10.1103/PhysRevApplied.15.054015>.
- [19] W. Liu et al. “Exciton dynamics at a single dislocation in GaN probed by picosecond time-resolved cathodoluminescence”. In: *Applied Physics Letters* 109.4 (July 2016), p. 042101. ISSN: 0003-6951. DOI: 10.1063/1.4959832. eprint: [https://pubs.aip.org/aip/apl/article-pdf/doi/10.1063/1.4959832/14483112/042101\\_1\\_online.pdf](https://pubs.aip.org/aip/apl/article-pdf/doi/10.1063/1.4959832/14483112/042101_1_online.pdf). URL: <https://doi.org/10.1063/1.4959832>.
- [20] A. Hangleiter et al. “Suppression of Nonradiative Recombination by V-Shaped Pits in GaInN/GaN Quantum Wells Produces a Large Increase in the Light Emission Efficiency”. In: *Phys. Rev. Lett.* 95 (12 Sept. 2005), p. 127402. DOI: 10.1103/PhysRevLett.95.127402. URL: <https://link.aps.org/doi/10.1103/PhysRevLett.95.127402>.
- [21] Idris A. Ajia et al. “Generated Carrier Dynamics in V-Pit-Enhanced InGaN/GaN Light-Emitting Diode”. In: *ACS Photonics* 5.3 (Mar. 2018), pp. 820–826. DOI: 10.1021/acsp Photonics.7b00944. URL: <https://doi.org/10.1021/acsp Photonics.7b00944>.
- [22] Huanyou Wang et al. “V-defects formation and optical properties of InGaN/GaN multiple quantum well LED grown on patterned sapphire substrate”. In: *Materials Science in Semiconductor Processing* 29 (2015). Special Topical Issue on Wide-Bandgap Semiconductor Materials, pp. 112–116. ISSN: 1369-8001. DOI: <https://doi.org/10.1016/j.mssp.2013.11.019>. URL: <https://www.sciencedirect.com/science/article/pii/S1369800113003545>.
- [23] Fatimah Alreshidi et al. “Enhanced Efficiency InGaN/GaN Multiple Quantum Well Structures via Strain Engineering and Ultrathin Subwells Formed by V-Pit Sidewalls”. In: *ACS Applied Optical Materials* 2.1 (Jan. 2024), pp. 220–229. DOI: 10.1021/acsaom.3c00406. URL: <https://doi.org/10.1021/acsaom.3c00406>.
- [24] Francois Olivier et al. “Shockley-Read-Hall and Auger non-radiative recombination in GaN based LEDs: A size effect study”. In: *Applied Physics Letters* 111 (July 2017), p. 022104. DOI: 10.1063/1.4993741.
- [25] H. W. Choi et al. “Mechanism of enhanced light output efficiency in InGaN-based microlight emitting diodes”. In: *Journal of Applied Physics* 93.10 (May 2003), pp. 5978–5982. ISSN: 0021-8979. DOI: 10.1063/1.1567803. eprint: [https://pubs.aip.org/aip/jap/article-pdf/93/10/5978/12243945/5978\\_1\\_1\\_online.pdf](https://pubs.aip.org/aip/jap/article-pdf/93/10/5978/12243945/5978_1_1_online.pdf). URL: <https://doi.org/10.1063/1.1567803>.
- [26] Palmerina González-Izquierdo et al. “Influence of Shape and Size on GaN/InGaN  $\mu$ LED Light Emission: A Competition between Sidewall Defects and Light Extraction Efficiency”. In: *ACS Photonics* 10.11 (2023), pp. 4031–4037. DOI: 10.1021/acsp Photonics.3c00971. eprint: <https://doi.org/10.1021/acsp Photonics.3c00971>. URL: <https://doi.org/10.1021/acsp Photonics.3c00971>.
- [27] Ryan T. Ley et al. “Revealing the importance of light extraction efficiency in InGaN/GaN microLEDs via chemical treatment and dielectric passivation”. In: *Applied Physics Letters* 116.25 (June 2020), p. 251104. ISSN: 0003-6951. DOI: 10.1063/5.0011651. eprint: [https://pubs.aip.org/aip/apl/article-pdf/doi/10.1063/5.0011651/13172538/251104\\_1\\_online.pdf](https://pubs.aip.org/aip/apl/article-pdf/doi/10.1063/5.0011651/13172538/251104_1_online.pdf). URL: <https://doi.org/10.1063/5.0011651>.
- [28] Jean Wei et al. “Measurement of temperature dependent refractive indices of GaN and 4H-SiC”. In: *Nonlinear Frequency Generation and Conversion: Materials and Devices XX*. Ed. by Peter G. Schunemann and Kenneth L. Schepler. Vol. 11670. International Society for Optics and Photonics. SPIE, 2021, 116700Q. DOI: 10.1117/12.2578411. URL: <https://doi.org/10.1117/12.2578411>.
- [29] Shuo-Wei Chen et al. “Effects of Nanoscale V-Shaped Pits on GaN-Based Light Emitting Diodes”. In: *Materials* 10.2 (2017), p. 113. ISSN: 1996-1944. DOI: 10.3390/ma10020113. URL: <https://www.mdpi.com/1996-1944/10/2/113>.
- [30] T. L. Song. “Strain relaxation due to V-pit formation in  $\text{In}_x\text{Ga}_{1-x}\text{N}$  GaN epilayers grown on sapphire”. In: *Journal of Applied Physics* 98.8 (Oct. 2005), p. 084906. ISSN: 0021-8979. DOI: 10.1063/1.2108148. eprint: [https://pubs.aip.org/aip/jap/article-pdf/doi/10.1063/1.2108148/13408390/084906\\_1\\_online.pdf](https://pubs.aip.org/aip/jap/article-pdf/doi/10.1063/1.2108148/13408390/084906_1_online.pdf). URL: <https://doi.org/10.1063/1.2108148>.
- [31] Tao Zhu, Liwen Cheng, and Xianghua Zeng. “Effect of V-pits size on the reliability of InGaN/GaN light emitting diodes”. In: *Superlattices and Microstructures* 157 (2021), p. 106990. ISSN: 0749-6036. DOI: <https://doi.org/10.1016/j.spmi.2021.106990>. URL: <https://doi.org/10.1016/j.spmi.2021.106990>.

[www.sciencedirect.com/science/article/pii/S0749603621001889](http://www.sciencedirect.com/science/article/pii/S0749603621001889).

- [32] Cheng-Han Ho et al. “Efficiency and Forward Voltage of Blue and Green Lateral LEDs with V-shaped Defects and Random Alloy Fluctuation in Quantum Wells”. In: *Phys. Rev. Appl.* 17 (1 2022), p. 014033. DOI: 10 . 1103 / PhysRevApplied . 17 . 014033. URL: <https://link.aps.org/doi/10.1103/PhysRevApplied.17.014033>.